Title: The relationship between microbiomes and selective regimes in the sponge genus *Ircinia*.

Authors: Joseph B. Kelly[1,2*], David Carlson[1], Jun Siong Low[3,4], Tyler Rice[4], Robert W. Thacker[1,5].

Affiliations:

[1]Stony Brook University, Department of Ecology and Evolution, Stony Brook NY, USA.

[2]Limnological Institute University Konstanz, Aquatic Ecology and Evolution, Konstanz, Germany.

[3]Fondazione per l'istituto di Ricerca in Biomedicina, Bellinzona, Switzerland.

[4]Department of Immunobiology, Yale University School of Medicine, New Haven, CT, USA.

[5]Smithsonian Tropical Research Institute, Box 0843-03092, Balboa, Republic of Panama.

*Correspondence to: joseph.b.kelly@stonybrook.edu.

Abstract

Sponges are often densely populated by microbes that benefit their hosts through nutrition and bioactive secondary metabolites; however, sponges must simultaneously contend with the toxicity of microbes and thwart microbial overgrowth. Despite these fundamental tenets of sponge biology, the patterns of selection in the host sponges' genomes that underlie tolerance and control of their microbiomes are still poorly understood. To elucidate these patterns of selection, we performed a population genetic analysis on multiple species of *Ircinia* from Belize, Florida, and Panama using an F_{ST}-outlier approach on transcriptome-annotated RADseq loci. As

part of the analysis, we delimited species boundaries among seven growth forms of *Ircinia*. Our analyses identified balancing selection in immunity genes that have implications for the hosts' tolerance of high densities of microbes. Additionally, our results support the hypothesis that each of the seven growth forms constitutes a distinct *Ircinia* species that is characterized by a unique microbiome. These results illuminate the evolutionary pathways that promote stable associations between host sponges and their microbiomes, and that potentially facilitate ecological divergence among *Ircinia* species.

Main Text

Introduction

Microorganisms affect nearly every aspect of macro-organismal biology. Across eukaryotes, the influences of microbiomes on hosts can be found in biological processes such as nutrition, development, and disease resistance [1–4]. These effects can be advantageous, for example, by producing essential nutrients for the hosts [5] and by enabling the exploitation of novel resources [6–8]. An important characteristic of metazoan microbiomes concerns their stability, or at the very least the prevention of their overgrowth of the host, as commensal microbes can transition into opportunistic pathogens [9]. The universal challenge of maintaining healthy associations with microbiomes is met by diverse strategies that include embargoes [10], phagocytosis [11], and physical expulsions of microbes [12]. Beneath the many mechanisms of microbiome control might lie a common process among metazoans that polices the crosstalk between hosts and their microbes: the innate immune system. This proposition is supported by observations that pathways concerned with innate immune surveillance, especially in

46 lipopolysaccharide (LPS) sensing, are functionally conserved across distantly related host clades.
47 LPS is a common membrane-motif found in nearly all gram-negative bacteria and has been
48 coopted as a prototypical endotoxin that binds to toll-like receptors (TLRs), instigating an
49 immune response. Interestingly, similarities have been documented between human and sponge
50 LPS-induced pathways, including the likely role of toll-like receptors (TLRs) as pattern
51 recognition receptors (PRRs) that bind LPS [13]. Furthermore, nodal signaling molecules
52 downstream of the LPS-induced pathway in humans, serine-threonine-directed mitogen-activated
53 protein kinases (MAPK) p38 kinases and c-*jun* N-terminal kinases/JNK [14], are also stimulated
54 by LPS in sponges [15], a clade that is among the most distant metazoan relatives of humans.
55 Given the homology between the components of the LPS-induced pathway, and the fact that
56 sponges and humans share a common ancestor at the base of the metazoan phylogeny [16], these
57 pathways might constitute extant versions of the innate immune system of ancient metazoans
58 that facilitated inhabitation of hosts by symbiotic microbes in Earth's early oceans, and which
59 promote stable associations between hosts and microbes today.
60 Sponges stand out as a holobiont success story. The relationship between sponges and
61 their microbes is a longstanding affair dating back to the advent of the phylum Porifera over 540
62 million years ago [17]. Symbiotic microbes can comprise a substantial physical portion of
63 sponge bodies, constituting up to 40% of the total biomass in some host species [18–20]. Much
64 like the zooxanthellae of coral, the cyanobacterial photosymbionts of sponges can supplement
65 the host's nutrition [4]; although in some sponges that possess high abundances of symbiotic
66 microbes, often termed high microbial abundance or HMA sponges, cyanobacteria only
67 constitute a portion of the microbial diversity [21]. The remaining fraction of these microbiomes
68 can be comprised of thousands of microbial species from dozens of bacterial phyla [21] that

perform fermentation [20], produce secondary metabolites [22], conduct chemoautotrophic processes such as nitrogen fixation and sulfur oxidation [23–25] and heterotrophic processes via the assimilation of dissolved organic matter (DOM) [26]. Based on measurements of nutrient transfer from microbes to their hosts [27], supplements of microbial origin to the sponges' energy pools that the hosts use for growth [4,28], and chemical defense by the secondary metabolites [29,30], microbial symbionts can be identified as influencing the fitness of their hosts in addition to shaping their ecological identities.

The importance of microbiomes to HMA sponges is reflected in the observation that they tend to be compositionally stable and distinct relative to the microbial communities of the surrounding environment [21,31]. The microbiomes can also be divergent among host species [21] which, combined with the metabolic diversity of the microbes, supports the hypothesis that the microbiome acts as a mechanism for ecological diversification within sponges. This evolutionary model has received some of its strongest support in recent work investigating the bulk isotopic enrichment levels of sympatric sponge species [32], where both microbiome compositions and isotopic enrichment values were divergent among host taxa within geographic sites, identifying the microbiomes as being not only a mechanism for accessing novel resources but also a means for alleviating resource competition. Granted that microbiomes hold the potential to unlock access to new resources, they might also enable ecological diversification among incipient sponge species.

A suitable case study to test this hypothesis exists in *Ircinia*, a cosmopolitan sponge genus comprised of over 130 described species, many of which are densely populated by taxonomically diverse communities of symbiotic microbes [33–36]. The microbiomes of several *Ircinia* are compositionally stable [33,37] and unique among host species (Kelly & Thacker 2020

92 A, *in review*). These microbes also have the potential to supplement host nutrition given the high
93 rates of primary productivity in Caribbean *Ircinia* [38] and isotopic evidence demonstrating the
94 allocation of microbial nitrogen to the hosts [39]. In the Caribbean, *Ircinia* are characterized by
95 divergence among the species' microbiome compositions, a feature that might underly local
96 adaptation (Kelly & Thacker 2020 A, *in review*). Thus, the present study sought to use Caribbean
97 *Ircinia* to investigate how patterns of selection in the hosts' genomes promote the residence of
98 symbiotic microbes which could, in turn, mediate ecological divergence among closely related
99 host species. To perform this study, we first tested whether active control of microbiomes by the
100 hosts is evidenced throughout *Ircinia* by characterizing beta diversity among the microbial
101 consortia of the hosts and surrounding seawater using 16S rRNA metabarcoding. Second, we
102 tested whether this control translates to dissimilar microbiome compositions among *Ircinia* host
103 species, several of which we delimited using 2bRAD (RADseq) data, as the possession of unique
104 microbiomes is congruent with prior evidence of ecological diversification within sponges [32].
105 Finally, we identified F_{ST} outliers in the 2bRAD data and annotated them using a *de novo*-
106 assembled and annotated transcriptome to find candidate genes that might underly divergence in
107 microbiome control, as well as genes that could facilitate the tolerance of symbionts.
108

109 ***Results***

110 *Microbial Communities*

111 To test whether the taxonomic compositions of *Ircinia* microbiomes are distinct relative
112 to the community compositions of the ambient seawater microbial community, and to test
113 whether the microbiome compositions are unique within each *Ircinia* growth form, we censused
114 the microbial communities of seawater samples and the microbiomes of *Ircinia* spp. by

115 sequencing the V4 region of the 16S rRNA gene. Relative abundance matrices of OTUs were
116 constructed using mothur v1.39.5 [40] with an OTU clustering threshold of 99%. Differences
117 among community compositions among groups (i.e. *Ircinia* and seawater) were inferred using
118 PERMANOVA based on Bray-Curtis dissimilarity [41]. Microbiome compositions among the
119 host *Ircinia* lineages (populations of nominal species and growth forms) were visualized using
120 principal coordinate analysis, and dissimilarities among the microbiome compositions of these
121 lineages were further investigated by calculating the average overlaps among the standard ellipse
122 areas (SEAs) of the data using SIBER [42].

123 Sequencing of 16S rRNA amplicons generated from the host *Ircinia* and seawater
124 samples generated 8,777,283 paired-end raw reads, of which trimmomatic removed 67.64% [43].
125 Of the remaining 2,839,911 reads, 2,000,318 survived downstream quality control steps
126 including removal of homopolymers and chimeric reads in mothur v1.39.5 [40] (Table S1). 392
127 OTUs were identified as chloroplasts and one OTU as mitochondrial. 11042 OTUs were
128 retrieved at the 99% clustering threshold, which SILVA v132 identified as belonging to 59
129 accepted and candidate prokaryotic phyla [44]. The mean final read abundance per specimen was
130 15127.09 +/- 7458.258 (1 SD).

131 The microbiomes of *Ircinia* were compositionally distinct relative to seawater microbial
132 communities (PERMANOVA: $R^2 = 0.41$, $p = 1e^{-04}$). *Ircinia* microbiomes were 1.45x as
133 taxonomically rich at the OTU level relative to seawater microbial communities and contained
134 1.56x as many source-specific OTUs relative to seawater microbial communities. The two
135 sources only overlapped by 1043 of the 11042 OTUs, with 6115 OTUs only found in *Ircinia* and
136 3908 OTUs found only in seawater; however, the relative abundances of the OTUs found in both
137 seawater and sponges were correlated with their source, where OTUs that were highly enriched

138 in sponges were nearly absent in seawater, and vice versa (PERMANOVA: R2= 0.44, P = 1e-04,
139 Figure 2). The shared OTUs were also the most numerically dominant in the total dataset. When
140 considering the fraction of OTUs found in the sponges, the shared OTUs had an average relative
141 abundance of $8.59e^{-04}$ +/- $4.04e^{-03}$(1 SD), an order of magnitude greater than the average relative
142 abundance of sponge-specific OTUs ($1.71e^{-05}$ +/- $1.25e^{-04}$ (1 SD)). The same trend held for the
143 seawater dataset, where the shared OTUs had a mean relative abundance of $8.3e^{-04}$ +/- $4.42e^{-03}$ (1
144 SD), an order of magnitude greater than the average relative abundance of seawater-specific
145 OTUs $3.35e^{-05}$ +/- SD $1.28e^{-04}$ (1 SD). 8 OTUs were identical to 16S rRNA sequences from
146 bacteria reported to be vertically transmitted in *I. felix*, all of which fell within the intersection of
147 the sponge and seawater datasets, 6 of which were in appreciably higher relative abundances in
148 sponges relative to seawater (Table S4, Figure 2).

149 Each sponge lineage (growth form and population of nominal species) harbored unique
150 microbiomes, evidenced by the significance of 66 of 67 pairwise PERMANOVAs (Table S5).
151 Additionally, the microbiome compositions of each host lineage occupied distinct multivariate
152 space, in which each of the standard ellipse areas (SEAs) of each host lineage had a mean
153 overlap of 2.38 +/- 6.11 % (Figure 3). Within the nominal species *I. strobilina* and *I. campana*,
154 geographically distant populations of conspecifics harbored significantly dissimilar microbiome
155 compositions (Table S5). 108 OTUs were found across all 10 host species and could thus be
156 considered 'core' microbiota of Caribbean *Ircinia*. One OTU that blasted to the vertically
157 transmitted symbiont 16S sequences was found across all 10 species, Otu00012, belonging to
158 *Constrictibacter* (Proteobacteria, Alphaproteobacteria, Puniceispirillales, Puniceispirillales
159 incertae sedis) [45]. Of the eight putatively vertically transmitted symbionts, Otu00012 had the
160 highest average relative abundance across all host species (Figure 2).

161 F_{ST} *Outliers*

162 We investigated patterns of selection among the growth forms and populations of
163 nominal species among *de novo*-assembled 2bRAD loci sourced from the host sponges using an
164 F_{st} outlier approach. Prior to assembly and subsequent analyses, the 2bRAD data was
165 decontaminated by removing reads that mapped to metagenome-assembled genomes (MAGs) of
166 symbiotic prokaryotes in Caribbean *Ircinia* (Kelly et al. 2020, *in review*) using bbsplit
167 (sourceforge.net/projects/bbmap/). A locus was identified as an outlier if it fell outside the 90%
168 confidence interval (CI) that was estimated via fsthet [46], or if it deviated significantly from a
169 model of neutral evolution inferred via BayeScan [47] using a 10% false discovery rate (FDR).
170 We then annotated the outlier loci by mapping them to a *de novo*-assembled and annotated
171 transcriptome that we produced from an *Ircinia* specimen of the Floridian ramose growth form.
172 The transcriptome was also subjected to contaminant removal by mapping reads to *Ircinia*
173 prokaryotic symbiont MAGs, and also using a kraken-based pipeline [48] and deconseq [49] (see
174 Materials and Methods).

175 A total of 118,948,690 single-end reads corresponding to *Alf1* restriction digests were
176 generated using the 2bRAD pipeline, with an average of 1,383,124.30 reads +/- 629,275.12 (1
177 SD) per specimen. After processing the reads with 2bRAD_trim_launch.pl
178 (https://github.com/z0on/2bRAD_denovo) and cutadapt [50], a total of 103,371,805 reads
179 remained with an average of 1,201,997.73 +/- 566,898.18 (1 SD) reads per specimen.
180 Contamination screening against the MAGs of symbiotic prokaryotes via bbsplit removed on
181 average 74.52% +/- 7.89% (1 SD) of reads per sample. Samples with less than 125,988.63 reads
182 (the per-sample mean of post-decontamination reads minus 1 SD) were omitted from further
183 analysis. 66 samples remained with an average of 360,502.20 +/- 180,813.27 (1 SD) reads per

184 sample (Table S1). Assembly of the 2bRAD data in STACKS [51] requiring that a SNP be
185 present in 75% of the populations and in half of the individuals per population produced 389
186 loci, 333 of which were variant, 50 of which were later identified as outliers by fsthet [46] and
187 BayeScan [47].

188 Decontamination of the transcriptomic data via kraken [48] removed 14.88% of reads and
189 bbsplit removed a further 0.49%. After *de novo* assembly in Trinity [52], deconseq [49] removed
190 3791 sequences corresponding to 1.84% of the assembled transcripts. The final assembled
191 transcriptome had a contig N50 of 1570 bps and a metazoan-specific BUSCO completeness
192 score of 95.6%, 191,399 transcripts, 126,897 Trinity "genes", and a GC content of 41.58 %.
193 51,471 transcripts received functional annotations via HMMER, implemented in dammit [53],
194 that met the e-value cutoff of <1e-5.

195 Fifty outlier loci were detected among the 333 variant 2bRAD loci; BayeScan identified
196 13, 10 of which were candidates for positive selection and 3 for balancing selection, and fsthet
197 identified 43, 18 of which for candidates for positive selection and 25 for balancing selection.
198 One locus identified as being under balancing selection and five outlier loci under positive
199 selection were detected by both methods. 18 of these loci mapped to the transcriptome and
200 passed the annotation criteria (Table 2). Two of the positively selected outliers mapped to genes
201 involved in cellular mechanics (FLNC and FLNB), and one to a gene involved in maintaining
202 DNA integrity (BLM). One of the genes under balancing selection is involved in protein
203 degradation (S8 Family Serine Peptidase), and five in host immune and stress responses
204 (MAP3K, Rassf1, TES, PRSS21, and Kdm5b). One of the positively selected loci mapped to a
205 mobile genetic element (TY3B-G) as did six loci under balancing selection (three POL, gag-pol,
206 GIY-YIG, pro-pol-dUTPase). Additionally, the two genes annotated as TES and PRSS21 also

207 contained viral recombination domains (phage integrase family); PRSS21 also contained a
208 reverse transcriptase domain.

209

210 *Species Boundaries and Gene Flow*

211 We delimited genetic species boundaries among *Ircinia* growth forms by performing a
212 multispecies coalescent-based test of genetic species boundaries using BFD* [54], a pipeline that
213 evaluates support among competing species-grouping hypotheses using Bayes factors [55].
214 BFD* also provides a suitable test of genetic species boundaries given our dataset as the pipeline
215 is robust to SNP under-sampling and the sampling of relatively few individuals per species [54].
216 Competing species-grouping models were constructed based on whether growth forms shared a
217 habitat type (e.g. mangrove, seagrass bed, coral reef), had similarities in the overall features of
218 their growth habit (e.g. encrusting, massive), or were sourced from the same or nearby sites
219 (Table 1). Additionally, we investigated patterns of hybridization among the species identified by
220 BFD* using STRUCTURE [56]. Prior to these analyses, F_{st} outliers that were identified by either
221 fsthet [46] or BayeScan [47] were removed to help ensure the assumption of neutrality was met
222 [57].

223 BFD* lent highest support to the model representing each growth form and population of
224 nominal species as a separate species (Table 1). The clades that were recovered via SNAPP
225 showed a strong correlation with geography, especially with the Panamanian populations, which
226 were monophyletic with the exception of *I. strobilina* (Figure 4). The Floridian and Panamanian
227 *I. campana* were divided into two distinct clades that were connected by a deep node near the
228 base of the tree; however, the *I. strobilina* populations were monophyletic.

229 The best supported number of ancestral populations was identified unambiguously as
230 K=4, followed distantly by K=5, by the Evanno method [56] (Figure S1). Both the K=4 and K=5
231 STRUCTURE plots showed patterns of hybridization indicative of interbreeding among *Ircinia*
232 species, with rates of hybridization greater within sites relative to across sites (Figure 5). In both
233 plots, SNPs from both populations of *I. strobilina* were predominantly sourced from a shared
234 ancestral population, whereas *I. campana* was split between two ancestral populations that
235 coincided with geography.

236

237 ***Discussion***

238 Our results provide the first insight into the selective forces on specific genes that might
239 underlie microbiome control and tolerance in high-microbial abundance (HMA) sponges. In
240 particular, balancing selection was detected in immune system genes and positive selection in
241 genes that concern the sponge's mechanical control of its body and DNA repair. A heritable
242 component of microbiome control might also be evidenced in our observations of dissimilarity
243 between host microbiomes and seawater microbial communities. Combined with previous
244 observations of vertical transmission of microbial symbionts in sponges [58–61] and the fitness
245 benefits to host sponges that can result from microbial farming [4,39], our study provides a
246 model that could help explain the persistence of host-microbial relationships throughout the
247 evolutionary history of Porifera.

248

249 *Hidden Species Richness of Caribbean Ircinia*

The growth forms of Caribbean *Ircinia* appear to be genetically distinct species, a hypothesis that held despite high rates of hybridization. Two notable features stand out on the species tree for the best-supported BFD* species model. The first is a strong correlation of the grouping of taxa with geography – all four Panamanian growth forms are monophyletic with the Panamanian population of *I. campana*, and the Floridian Ramose growth form is monophyletic with the Floridian population of *I. campana*. Second, and perhaps more striking, is the polyphyly of the *I. campana* populations. Conversely, the allopatric populations of *I. strobilina* are monophyletic on the tree.

Sympatric sister lineages on the phylogeny are separated by nodes as deep or deeper than the one connecting the allopatric *I. strobilina* populations (see the pairs of sister lineages: *I. campana* Florida and Ramose and Massive A pink vs Encrusting, Figure 4). We interpret the BFD* results, the depths of these nodes, and the distinct physical characteristics of each growth form as support for the hypothesis that each growth form represents a separate species, despite high rates of hybridization. We recommend further investigation into the taxonomy of *I. campana* as our results provide evidence that this taxon likely consists of multiple species. We recommend against splitting *I. strobilina* into two species; we interpret the observed divergence among samples as population-level differences, based on comparisons of the depth of the node joining the two allopatric *I. strobilina* populations to the depths of nodes joining sympatric species pairs. Complete scientific descriptions of each of these species are provided in a separate publication (Kelly & Thacker 2020 B, *in review*).

Microbiome Compositions of Caribbean Ircinia are Distinct from Seawater Microbial Communities and are Unique among Host Species

Consistent with prior observations (Kelly & Thacker 2020 A, *in review*), the most abundant microbes are those shared between host and seawater, whereas the OTUs specific to either sponges or seawater occur in relatively low abundances. None of these shared OTUs co-occurred in high relative abundances in both sources. Instead, sponges appear to be actively excluding some microbes that occur in high abundances in seawater and fostering high relative abundances of microbes that are only found in trace abundances in seawater. The presence of the majority of putatively vertically transmitted microbes in the set of microbes being maintained at high relative abundances in sponges supports this finding.

The microbiomes of each *Ircinia* host lineage are unique with regard to taxonomic composition, as the pairwise comparisons of the microbiome compositions of all allopatric species pairs and all but one sympatric species pairs were significantly dissimilar. Combined with the distinctiveness of the compositions of sponge microbiomes relative to the seawater microbial communities, a plausible explanation might be that a heritable mechanism in the sponges underlies microbiome assembly and potentially facilitates character displacement among sympatric species in addition to local adaptation to different habitats. Under the assumption that these microbes have an impact on the fitness of their hosts, which is a likely prospect given the high concentrations of photosynthetic pigments [62] and the presence of nitrogen metabolism [24] found in Caribbean *Ircinia*, these observations fit a model whereby microbiomes provide a conduit for ecological diversification within this genus.

292 The microbiomes of *Ircinia* species are also likely shaped on short-term ecological
293 timescales to some degree; however, data describing the responses of microbiome compositions
294 in Caribbean *Ircinia* to contrasting abiotic and biotic regimes across spatial and temporal scales
295 are in short supply and were predominantly collected from *Ircinia* inhabiting other ocean basins.
296 One study examining the Great Barrier Reef sponge, *I. ramosa*, found that microbiome
297 compositions were stable when exposed to different salinity regimes [63]. Additionally, previous
298 studies focusing on Mediterranean *Ircinia* spp. discovered that microbiome demographics are
299 stable within a host species across seasons and throughout the range of their species distributions
300 [33,37]. Recently, an analogous study was performed in the Caribbean that investigated patterns
301 of beta diversity among the microbiomes of *I. campana* populations [35]. This study discovered
302 a distance-decay relationship among the microbiome compositions of the populations [35],
303 which is consistent with the significantly dissimilar microbiome compositions of the *I. campana*
304 populations in the current study. However, given the topology of our species tree and the BFD*
305 results, it may be the case that more than one *Ircinia* species were investigated by the
306 aforementioned study, again confounding interpretations of the relative contributions of species-
307 level ecological divergence and ecological factors that scale with latitude. To better understand
308 how intersecting evolutionary and ecological forces dictate microbiome assembly in Caribbean
309 *Ircinia*, we advocate for more studies performing long-term monitoring of microbiome
310 compositions in Caribbean *Ircinia* and reciprocal transplant experiments that could help
311 elucidate how *Ircinia* are able to use their microbiomes to exploit unique resource pools in
312 different habitats.

313

314 *The Role of Selection in Ircinia Evolution*

315 The demands of living in a microbial world must be met by competent host defenses.
316 Immune system genes are routinely subjects of balancing selection given the positive effect
317 allelic diversity has in guarding against novel cellular assaults and in detecting a broader suite of
318 foreign epitopes [64], and have been previously detected as being under balancing selection in
319 sponges [65]. In our dataset, we detected multiple outliers under balancing selection involved in
320 immune responses. The first two, MAP3K and Rassf1, are both expressed in the cytosol and are
321 components of the Ras-Raf-MEK-ERK (MAPK/ERK) LPS-induced pathway that communicates
322 molecular signals of a bacterial infection to drive the transcriptional changes necessary for an
323 immune response [66]. This signaling pathway also plays a role in cell-cycle mediation and in
324 the induction of apoptosis, and is thought to be tumor-suppressing given the silencing of Rassf1
325 and somatic mutation of MAP3K in many cancers [67–70]. Two other oncogenes under
326 balancing selection are TES (testisin) and PRSS21 (testisin precursor). Both are localized in the
327 cell membrane. The former is a focal adhesion protein that controls cell proliferation [71], the
328 latter, a serine protease that is putatively involved in the regulation of proteolysis during germ
329 line development [72]. Our analysis detected both positive and balancing selection in biological
330 processes involved in maintaining DNA integrity. Balancing selection was detected in Kdm5b, a
331 histone demethylase expressed in the nucleus that signals double-stranded breaks in DNA [73].
332 Balancing selection was also detected in a member of the GIY-YIG nuclease family, which
333 includes members that prevent the incorporation of exogenous DNA and are thought to preserve
334 DNA integrity in basal metazoans [74,75]. Positive selection was detected in the BLM protein,
335 which helps ensure accurate recombination during double-strand DNA break repair [76].

336 The concentration of bioactive compounds in *Ircinia* can be substantial, and some that
337 have been identified as being produced by the symbiotic microbes are cytotoxic [77–79]. Many

338 prokaryotic symbionts present in the adult sponges have also been observed in *Ircinia* larvae,
339 where the toxic effects of the secondary metabolites are likely pronounced [58]. Thus, balancing
340 selection in immune system genes could be having a fitness effect in multiple cellular
341 compartments (cell membrane, cytosol, and nucleus) and over the lifespan of the host.
342 Additionally, the patterns of selection present in genes that promote DNA integrity, including
343 oncogenes, could result in adaptations to the molecular apparatuses that prevent mutagenesis of
344 host DNA in an environment that contains abundant foreign DNA and secondary metabolites.

345 Both balancing and positive selection were detected in viral recombination genes,
346 providing the second account of selection in genes of a viral origin in sponge hosts [65].
347 Additionally, a recent study investigating the roles of phages in sponge symbionts discovered
348 that bacteriophages of four Mediterranean sponge species contain ankyrin repeats, which likely
349 aid the symbiont in evasion of the host's immune system, and other genes that supplement the
350 host bacterium's metabolism [80]. Since similar viral loci are under selection in the host, it may
351 be the case that viruses are also transferring adaptive gene content to the sponges. Another
352 biologically plausible scenario is that these genes are erroneously being detected as under
353 selection, in that if they are in close proximity to other genes that are the true targets of selection,
354 then our analysis could be detecting them as a result of a hitchhiking effect. However, this
355 scenario does not preclude the possibility that the viral loci might still somehow be involved in
356 the mobility of the target of selection. Further research that can provide information on the
357 physical relationship among these loci (i.e. using a reference genome) is required to better vet the
358 potential for viruses to introduce adaptive genes to host sponges.

359 Two of the loci under positive selection (FLNC and FLNB) are involved in cellular
360 mechanics, including the development and functioning of muscles in other metazoans [81–83];

361 additionally, the copy of FLNC in our dataset contains a CH-like domain that is present in sperm
362 flagella (Table 2). These genes might be involved in contractions of the canal system and the
363 mechanics of the flagellar beating of the choanocytes, which regulate the flow of water
364 throughout the sponge [84]. Some host organisms, such as legumes, control their microbiome by
365 manipulating the microenvironment, which can deprive root nodules that are overgrown with
366 cheater strains of rhizobia of oxygen [10]. Sponges might control their microbiomes analogously,
367 as they are able to control which portions of their aquiferous canal system receive irrigation,
368 resulting in a heterogenous distribution of oxygen that could impact physiologies of bacterial
369 symbionts and thus change the microbiome composition [85]. Given that the growth forms are
370 specific with regard to habitat preference, the divergence among these genes could further be
371 compounded by the different hydrodynamic environments of coral reefs, seagrass beds, and
372 mangroves [86].

373

374 ***Conclusion***

375 Ecological divergence, as facilitated by the microbiomes of Caribbean *Ircinia*, could be
376 enabled in part by the patterns of selection we detected in the genomes of the hosts, which
377 include balancing selection at immunity genes and positive selection in genes involved in
378 cellular mechanics and the maintenance of DNA integrity. Of special interest are the immunity
379 genes, as the innate immune system of sponges might play a central role governing host-
380 microbial crosstalk and maintaining a healthy microbial homeostasis [87]. Immunity pathways
381 involving the mitogen-activated protein kinases (MAPKs) p38 protein kinase and c-*jun* N-
382 terminal kinases/JNK are induced by LPS in the model sponge species *Suberites domuncula* [15].

383 One of the pathways detected as being under balancing selection here, Ras-Raf-MEK-ERK
384 (MAPK/ERK), is stimulated by LPS in human cell lines and triggers downstream immune
385 responses from the host [14]. Given the conservation of the actions of the other two MAPK
386 pathways, a similar biological function could perhaps be performed by MAPK/ERK in *Ircinia*.
387 Future work should test whether this pathway is inducible by microbes or microbial metabolites
388 and investigate the implications of its role in the cell cycle for tolerance of the microbiome. By
389 identifying the products of genes in this pathway and of other genes that we detected as being
390 under selection, such research will further illuminate how sponges coexist with their
391 microbiomes and how selection in the host genome might drive microbially mediated ecological
392 diversification.
393

394 ***Materials and Methods***

395 *Specimen collections and next generation sequencing library preparation*

396 Specimens of *Ircinia* representing seven growth forms were collected from three sites:
397 Bocas del Toro, Panama (July 2016), the Florida Keys (July 2018), and the Mesoamerican
398 Barrier Reef (August 2018) (Figure 1, Table S1). In Panama, individuals of the growth form
399 Massive A pink were collected form mangrove prop roots of *Rhizophora* at Inner Solarte;
400 individuals of two growth forms, Massive A green and Massive B, were collected from the
401 seagrass-dominated (*Thalassia*) habitat of STRI point; and individuals of the Encrusting growth
402 form were collected from patch reefs of Punta Caracol. In Florida, specimens of *I. campana* and
403 a growth form with a branching body morphology (Ramose) were collected from a 150 m-long
404 seagrass bed that begins 50 m immediately to the west of MOTE Marine Laboratory and
405 Aquarium's Elizabeth Moore International Center for Coral Reef Research & Restoration; *I.*

406 *campana* specimens were also collected from the coral reef at Looe Key. An additional specimen
407 of the Ramose growth form was snap frozen in an EtOH - dry ice bath and stored at -80C for
408 subsequent RNA extraction. In Belize, specimens of *I. strobilina* and *I. felix* were collected from
409 the forereef on the western (seaward) slope of Carrie Bow Cay. Specimens were collected of a
410 sixth growth form with an irregularly massive body morphology (Sp. 1) from the *Rhizophora*
411 prop roots of the Twin Cays and Blue Ground mangrove hammocks, and of a seventh growth
412 form with an encrusting body morphology (Sp. 2) from the Blue Ground coral patch reef.
413 Specimens of *I. strobilina* were also collected from the Blue Ground patch reef alongside Sp. 2.
414 All growth forms are specific with regard to habitat preference and inhabit either coral patch
415 reefs, seagrass beds, or mangrove prop roots, and were collected in close proximity to each other
416 within a site; all Panamanian collections were made within a 10.7-km radius, the Floridan
417 specimens shared a habitat, and the Belizean sampling locations fall within a 7.5-km radius.

418 Sponge specimens were fixed in 90% EtOH, which was replaced at the 24-hour and 48-
419 hour marks. 0.5L seawater specimens were taken immediately adjacent to the sampled *Ircinia* in
420 Panama and transported in opaque brown Nalgene bottles, subsequently concentrated via
421 vacuum filtration through 0.2-µm Whatman filter papers, and then stored in RNA later. DNA
422 extractions were made from the outermost 2mm layer of the sponge tissues using DNeasy
423 PowerSoil Kit (Qiagen) and from the interior of the sponge tissue (<2mm from the exterior
424 pinacoderm) and the seawater filter papers using the Wizard Genomic DNA Purification Kit
425 (Promega).

426 To census the taxonomic microbial community compositions of sponges and seawater,
427 we amplified the V4 region of the 16S rRNA (ribosomal subunit) from the DNeasy PowerSoil
428 Kit DNA isolations using the primers 515f (5' GTG YCA GCM GCC GCG GTA A 3') and

429 806rB (5' GGA CTA CNV GGG TWT CTA AT 3') following the Earth Microbiome Project
430 16S protocol (http://press.igsb.anl.gov/earthmicrobiome/protocols-and-standards/16s/). PCR
431 reactions were conducted in 50 uL volumes with the following recipe: 25 uL of 2x HotStarTaq
432 Master Mix, 1 uL of each primer at 10 uM concentration, 22 uL H_20, and 1 uL DNA template.
433 Thermocycler conditions used an initial denaturing step of 95°C for 5 minutes followed by 35 of
434 the following cycles: 94°C for 45 seconds, 50°C for 1 minute, and 72°C for 1.5 minutes; and was
435 completed with a final elongation step of 72°C for 10 minutes.

436 To generate genome-wide SNPs data for the host sponges, we constructed a 2bRAD
437 (RADseq) library from the sponge DNA isolations produced using the Genomic DNA
438 Purification Kit following the workflow of Wang et al. 2012 [88]**,** whereby all *Alf1* restriction
439 sites were targeted for amplification with the primers 5ILL-NN (5' CTA CAC GAC GCT CTT
440 CCG ATC TNN 3') and 3ILL-NN (5' CAG ACG TGT GCT CTT CCG ATC TNN 3') [88]. The
441 16S and 2bRAD libraries were multiplexed using 12-basepair Golay barcodes and pooled within
442 each amplicon type following dsDNA quantification on a Qubit 3.0.

443 RNA was extracted from the frozen Ramose specimen by incubating a homogenized
444 tissue fragment in Trizol and processing the resultant aqueous phase through the QIAGEN
445 RNAeasy kit following the manufacturer's instructions. The RNA extraction was sent to the Yale
446 Center for Genome Analysis (YCGA) for library preparation via poly-A pulldown and
447 sequencing on a NovaSeq6000. The 16S rRNA library was sequenced on a MiSeq in the lab of
448 Dr. Noah Palm at Yale University using a V2 2x250 bp chemistry kit, and the 2bRAD library
449 was sequenced on a NovaSeq 6000 at YCGA.

450

451 *Read Preprocessing and Data Hygiene*

452 Initial quality filtering was performed on the 16S rRNA reads using the paired-end
453 function in Trimmomatic v0.36 with the settings TRAILING:30 SLIDINGWINDOW:5:20
454 MINLEN:100 [43]. The forward 2bRAD reads were trimmed to the 36-bp restriction fragments
455 using the script 2bRAD_trim_launch.pl (https://github.com/z0on/2bRAD_GATK), and quality
456 filtered using cutadapt with the settings -q 15,15 -m 36 [50]. Decontamination of the 2bRAD
457 dataset (i.e. removal of reads of prokaryotic origin) was performed using bbsplit.sh
458 (https://sourceforge.net/projects/bbmap) with default mapping parameters against a reference
459 database of 356 metagenome-assembled genomes (MAGs) sourced from the same 12 *Ircinia*
460 host lineages studied here (Kelly et al. 2020, *in review*). RNAseq reads were filtered and
461 trimmed prior to assembly using the paired-end function of fastp v0.19.6 with the options --
462 poly_g_min_len 10 -x --poly_x_min_len 10 [89]. A first round of contaminant removal was
463 performed on the RNAseq data using kraken v1.1.1 with the parameter setting --confidence 0.05
464 [48]. To mitigate contamination of both eukaryotic and prokaryotic commensals, we
465 supplemented the default kraken databases with custom databases built from the aforementioned
466 dereplicated MAG dataset of *Ircinia* and a set of publicly available genomes downloaded from
467 NCBI, which is predominantly crustacean and annelid as these taxa comprised the majority of
468 eukaryotic commensals in the ramose growth form (Table S2). A second round of contaminant
469 removal was performed using bbsplit.sh, implemented with a modification to default mapping
470 parameters of maxindel=200000 and a reference database of the dereplicated *Ircinia* MAG
471 dataset.

472

473 *16S rRNA Analysis*

474 16S rRNA reads passing initial quality filters were assembled into contigs,
475 demultiplexed, and aligned to the V4 region of the SILVA v132 SSU reference sequence
476 database in mothur v1.39.5 [40]. Following removal of chimeric sequences, OTUs were
477 clustered at the 99% threshold using distance-based greedy clustering implemented in
478 VSEARCH [90]. OTUs represented by only one or two reads were omitted from the final dataset
479 to mitigate read error and contamination. Additionally, OTUs that were identified by SILVA as
480 being from mitochondria, chloroplasts, or Eukaryotes were removed from the dataset prior to
481 downstream analyses. To infer which OTUs might be vertically transmitted, we used BLASTn to
482 match the representative 16S rRNA sequences of our OTUs to a database of 16SrRNA sequences
483 from bacteria that are putatively vertically transmitted in *I. felix* [58], downloaded from NCBI
484 (Table S3). OTUs were identified as being putatively vertically transmitted if they had 100%
485 sequence identity over the entire length of the query.

486 Beta diversity among the host species and differences in microbial community
487 compositions between sponges and water were inferred using Permutational Analysis of
488 Variance (PERMANOVA) based on Bray-Curtis dissimilarity [41,91]. Sponge microbiome
489 compositions were visualized in multivariate space using a PCoA, and the overlap among the
490 standard ellipse areas of each host species' microbiome composition was calculated using SIBER
491 [42]. The number of unique and shared OTUs between seawater and sponge microbial
492 communities were plotted with the eulerr package (https://github.com/jolars/eulerr). Since
493 seawater microbial communities were not sampled from Florida, analyses comparing sponge and
494 seawater microbial communities are restricted to Panamanian and Belizean samples.

495

496 *Transcriptome Assembly, Post-Assembly Decontamination, and Functional Annotation*

497 Reads passing the kraken and bbsplit.sh filtering steps were *de novo* assembled using
498 Trinity v2.8.5 [52]. After assembly, a third round of contamination removal was performed using
499 deconseq v0.4.3 with default parameters and the publicly available mouse, human, bacterial,
500 archaeal, and viral deconseq reference databases [92]. Functional annotations were then made for
501 the assembly using the annotate function of dammit v1.0rc2 (https://github.com/dib-lab/dammit)
502 including the UniRef90 annotations (--full) and the metazoan lineage-specific BUSCO group
503 [53].

504

505 *De novo 2bRAD assembly*

506 Following parameter optimization via the guidelines of Paris et al. [93], we assembled the
507 2bRAD reads into loci *de novo* in Stacks v2.41 with the settings -m 3 -M 3 -n 4 [51].
508 Additionally, we filtered the data to require that a SNP be present in 75% of the populations (-p
509 9) and half of the individuals of a population (-r 0.50). For downstream population genetic
510 analyses, we used only the first variant site from each 2bRAD locus to satisfy the assumption of
511 independence among our SNPs.

512

513 F_{ST} *Outlier Detection and Annotation*

514 Using two methods, we detected F_{ST} outliers by treating each growth form and allopatric
515 population of nominal species as a separate population. First, via BayeScan v2.1, a Bayesian

516 software program that employs reversible-jump Monte Carlo Markov chains to estimate
517 posterior distributions of F_{ST} values for loci under two alternative models, one with selection and
518 another under neutral evolution [47]. Loci with posterior F_{ST} values that deviate from
519 expectations under the neutral model are identified as outliers. BayeScan was run for 5000
520 iterations with a thinning interval of 10 and a burn-in of 50000. Outliers were identified from the
521 output files and plotted using the R function plot_bayescan with a false discovery rate (FDR) of
522 0.10. Second, we identified outliers using the R package fsthet, an implementation of the F_{ST}-
523 heterozygosity approach of Beaumont & Nichols (1996) that identifies outlier loci against
524 smoothed quantiles generated from the empirical SNP dataset [46]. Using this approach, a given
525 locus was identified as an outlier if it fell outside the 90% confidence interval (CI) of its
526 heterozygosity bin.

527 To investigate the biological implications of selection in our dataset, we performed a two-
528 step functional annotation. First, we mapped 2bRAD loci containing outliers by querying them
529 against the assembled and annotated transcriptome using BLASTn with an e-value cutoff of 1e-
530 9. Functional annotations of transcripts containing outlier loci were deemed reliable if the
531 HMMER hits had e-values below 1e-5. Second, we queried outliers via BLASTx to the to the
532 NCBI non-redundant (nr) protein sequences database.

533

534 *Species Delimitation, Species Tree Estimation, and Hybridization*

535 SNPs that were identified as F_{ST} outliers were removed from the SNP matrix prior to
536 downstream population genetic analyses. Species delimitation was performed using Bayes factor
537 delimitation with genomic data (BFD*) [54]. 13 competing species grouping models were

538 constructed based on plausible biological scenarios (Table 1). Each model was assigned an alpha
539 = 1 and beta = 130 for the expected divergence prior θ and a prior distribution of gamma (2,200)
540 for the birth rate prior λ (https://www.beast2.org/bfd/). Marginal likelihoods were then estimated
541 for each competing model via path sampling analysis [95], which was run for 50,000 generations
542 with 28 path steps and a pre-burn-in of 25,000 generations. Bayes Factors were calculated and
543 compared following Kass & Raftery [55]. A species tree was estimated in SNAPP v1.3.0 for the
544 best-supported species grouping model using four MCMC chains, each with a length of 1 million
545 generations and a burn-in of 25% (totaling 3 million generations post-burn-in) [96]. Likelihood
546 estimates and trees were logged every 500 generations for the SNAPP species tree and the path
547 sampling analyses. Hybridization was inferred among the species identified by BFD* using
548 STRUCTURE by setting the number of ancestral populatiions (*K*) to range from 3 to 12 and
549 performing 10 runs for each *K* using an MCMC length of 200,000 and a burn-in of 50,000
550 generations [56]. *ΔK* was calculated to estimate the number of ancestral populations using the
551 Evanno method implemented in Structure Harvester v0.6.94 [56,97].

552

553 ***Data accessibility statement:***

554 The quality-controlled 16S rRNA, 2bRAD, and transcriptomic sequence data are deposited under
555 the GenBank accession numbers XXX, YYY, ZZZ, respectively.

556

557 ***Acknowledgements*:** We thank Dr. Jackie L. Collier and Dr. Liliana Davalos-Alvarez for their
558 comments on the manuscript; the staffs of the Smithsonian Tropical Research Institute's Bocas
559 Research Station, the Smithsonian's Carrie Bow Cay Field Station, and the MOTE Marine

560 Laboratory and Aquarium's Elizabeth Moore International Center for Coral Reef Research &
561 Restoration for their support on logistical aspects of the field work; and Barrett Brooks and Dr.
562 Karen Koltes for help with specimen collections in Carrie Bow Cay. We thank Dr. Noah Palm of
563 Yale University for use of his laboratory's MiSeq, and to the Yale Center for Genome Analysis
564 for their careful attention to the 2bRAD and RNA sequencing. This study was supported by a
565 Fellowship of Graduate Student Travel (Society for Integrative and Comparative Biology) and
566 Dr. David F. Ludwig Memorial Student Travel Scholarship (Association for Environmental
567 Health and Sciences Foundation) awarded to J.B.K. and by grants awarded to R.W.T. from the
568 U.S. National Science Foundation (DEB-1622398, DEB-1623837, OCE-1756249).

569

570 ***Competing interests*:** The authors have no competing interests to declare.

571

572 ***Table and Figure Captions***

573

574 **Table 1.** Bayes factor delimitation results. Rank corresponds to relative support via Bayes factor.

575

576 **Table 2.** Table listing F_{ST} outliers mapped to annotated transcripts.

577

578 **Figure 1: Top:** Four Panamanian growth forms were collected from three sites: Massive A pink
579 was collected from *Rhizophora* prop roots at Inner Solarte, a network of mangrove hammocks;

580 Massive A green and Massive B were collected from STRI Point, a *Thalassia* seagrass-
581 dominated habitat; and Encrusting was collected from Punta Caracol, a coral patch reef. *I.*
582 *campana* and *I. strobilina* specimens were also collected from STRI Point and Punta Caracol.
583 **Middle:** specimens of a growth form (Ramose) and *I. campana* were collected from a seagrass
584 bed on Summerland Key, Florida; two specimens of *I. campana* were also collected from Looe
585 Key. **Bottom:** Two Belizean growth forms were collected from three sites: Sp. 1 specimens were
586 collected from *Rhizophora* prop roots at the Twin Cays and from mangrove hammocks adjacent
587 to the series of Blue Ground coral patch reefs; and Sp. 2 specimens were collected from the coral
588 reefs at Blue Ground. Specimens of *I. strobilina* were collected form the same patch reef
589 inhabited by Sp. 2 and also from the forereef at Carrie Bow Cay, and *I. felix* specimens were
590 collected from the Carrie Bow Cay forereef. A complete sampling overview can be found in
591 Table S1.

592

593 **Figure 2. A:** plot showing the relative abundances of the 1043 OTUs that are shared between
594 sponges and seawater, restricted to Panama and Belize. Orange dots are relative abundances in
595 sponges, blue dots are relative abundances in seawater. Black triangles mark OTUs that
596 correspond to vertically transmitted bacteria in *I. felix* [58]. **B:** Venn diagram showing the
597 number of sponge-specific OTUs, seawater-specific OTUs, and OTUs found in both sources.
598 OTUs in the intersection of the two sources are plotted by relative abundance in A.

599

600 **Figure 3.** PCoA of microbiome compositions, normalized by relative abundance, for each host
601 lineage. Ellipses are standard ellipse area (SEA). Squares are Floridian specimens (FL), circles
602 are Panamanian specimens (PA), and triangles are Belizean specimens (BZ).

603

604 **Figure 4.** Phylogeny produced via SNAPP for the best-supported species grouping model in
605 BFD*. **Left:** consensus tree with posterior probabilities as node labels. **Right:** Densitree
606 visualization of posterior tree distribution displaying most frequent topology in blue and
607 alternative topologies in green and red. Tip labels are colored by geography: blue for Belize,
608 yellow for Florida, and red for Panama.

609

610 **Figure 5.** STRUCTURE plots of SNP ancestries estimated for K=4 and K=5.

611

612 **Figure S1.** Estimation of delta K using Structure Harvester.

613

614

615 **Table 1. The species model representing each growth from and each population of nominal**
616 **species as a distinct species (in bold letter face) received decisive support over competing**
617 **models.**

Species Model	Motivation	# Species	MLE	BF	Rank
all growth forms separate species, split I. campana and *I. strobilina* by geography	**Test population-level divergence.**	**12**	**-10712.77**	**2559.69**	**1**
split *I. campana* and *I. strobilina* by geography, combine Massive A pink and Panamanian *I. campana*	Test if Massive A pink is a Panamanian I. campana phenotype	11	-10723.72	2537.80	2
all growth forms separate species, split *I. campana* by geography	Test population-level divergence.	11	-10743.48	2498.29	3
split *I. campana* and *I. strobilina* by geography, combine Massive B and Panamanian *I. campana*	Test if Massive B is a Panamanian I. campana phenotype	11	-10743.96	2497.31	4
split *I. campana* and *I. strobilina* by geography, combine Encrusting and Panamanian *I. campana*	Test if Encrusting is a Panamanian I. campana phenotype	11	-10745.95	2493.33	5
split *I. campana* and *I. strobilina* by geography, combine Encrusting, Massive A pink, and Panamanian *I. campana*	Test if Encrusting and Massive A pink are Panamanian I. campana phenotypes	10	-10753.99	2477.27	6
split *I. campana* and *I. strobilina* by geography, split Massive B between Panamanian *I. campana* and Encrusting (reference Kelly & Thacker 2020 A)	Test if Massive B is a mixture of Encrusting and Panamanian *I. campana*	11	-10767.13	2450.98	7

split *I. campana* and *I. strobilina* by geography, combine Massive A pink, Massive B, Encrusting, and Panamanian *I. campana*	Test if Massive B, Encrusting, and Massive A pink are Panamanian *I. campana* phenotypes	9	-10779.35	2426.54	8
split *I. campana* and *I. strobilina* by geography, combine sp2 and Belizean *I. strobilina*	Test if sp 2 is a Belizean *I. strobilina* phenotype	11	-10809.40	2366.44	9
all growth forms separate species, split *I. strobilina* by geography	Test population-level divergence.	11	-10895.09	2195.06	10
all growth forms separate species, combine *I. campana* and *I. stroblinia* populations	Full species model combining populations of nominal species.	10	-10924.28	2136.68	11
combineMassive A pink and Massive B	Both massive; shared geography.	9	-10940.90	2103.44	12
combine Massive B and Massive A green	Shared habitat (STRI point); sympatry.	9	-10942.36	2100.53	13
combine Massive A green and Encrusting	Sympatry	9	-10990.90	2003.45	14
combines sp1 and Massive A pink	Shared habitat type (mangrove)	9	-11064.83	1855.58	15
combine ramose and *I. campana*	Sympatry	9	-11073.93	1837.39	16
combine sp2 and Encrusting	Shared habitat type (coral patch reef)	9	-11224.58	1536.08	17
combine sp1 and sp2	Sympatry	9	-11357.66	1269.93	18
combine growth forms into one species	Are the growth forms different phenotypes of the same species?	4	-11826.39	332.46	19

combine growth forms with *I. felix*	Are the growth forms different *I. felix* phenotypes?	3	-11992.62	-	20

618

619 **Table 2. Outliers mapped to annotated transcripts. Transcripts with identical annotations**
620 **are collapsed into one row. Genes involved in immunity are under balancing selection and**
621 **genes involved in cellular mechanics are under positive selection in *Ircinia*.**

BayeScan	fsthet	2bRAD Locus Outlier	Trinity 'gene'	Transcripts on gene	Domain features via HMMER	Gene annotation via NCBI
positive sel		CLocus_76203	TRINITY_DN2919_c0_g1	Transcript_19655	CH-like domain in sperm protein, CAMSAP CH domain, Filamin/ABP280 repeat, Cyclin N-terminal domain	FLNC
	balancing sel	CLocus_376757	TRINITY_DN3714_c0_g1	Transcript_24274, Transcript_24276, Transcript_24277,	Ras association (RalGDS/AF-6) domain, Novel Ras effector 1 C-terminal SARAH (Sav/Rassf/Hpo) domain, Ankyrin repeats (Ank,	Rassf1

				Transcript_24278, Transcript_24279	Ank_2, Ank_3, Ank_4, Ank_5)	
	balancing sel	CLocus_228457	TRINITY_DN13274_c0_g1	Transcript_67503, Transcript_67504	Reverse transcriptase-like	POL
positive sel	positive sel	CLocus_13857	TRINITY_DN17238_c0_g1	Transcript_78835	Integrase core domain, Reverse transcriptase (RNA-dependent DNA polymerase), Zinc knuckle	TY3B-G
	balancing sel	CLocus_219329	TRINITY_DN23900_c0_g2	Transcript_93043	Phage integrase family	TES
	balancing sel	CLocus_685090	TRINITY_DN1258_c2_g1	Transcript_9588, Transcript_9591, Transcript_9594	PHD-finger	Kdm5b
positive sel		CLocus_76713	TRINITY_DN1384_c0_g1	Transcript_9901, Transcript_9903	Filamin/ABP280 repeat, YtkA-like	FLNB

	balancing sel	CLocus_223903	TRINITY_DN2279_c0_g2	Transcript_15199	Reverse transcriptase (RNA-dependent DNA polymerase)	GIY-YIG
	balancing sel	CLocus_32978	TRINITY_DN7718_c0_g1	Transcript_45973	BED zinc finger	ZBED4
	positive sel	CLocus_13672	TRINITY_DN11504_c0_g1	Transcript_61643, Transcript_61644	DEAD/DEAH box helicase, Helicase conserved C-terminal domain	BLM
	balancing sel	CLocus_31257	TRINITY_DN12087_c0_g1	Transcript_63383, Transcript_63384, Transcript_63390	no sig. HMMER hits	S8 Family Serine Peptidase
	balancing sel	CLocus_214786	TRINITY_DN23991_c0_g1	Transcript_93163	Integrase core domain	POL
	balancing sel	CLocus_34684	TRINITY_DN68288_c0_g1	Transcript_136651, Transcript_136653, Transcript_136654, Transcript_136655, Transcript_136656	Phage integrase family, Reverse transcriptase (RNA-dependent DNA polymerase)	PRSS21

	balancing sel	CLocus_234266	TRINITY_DN185_c0_g1	Transcript_1675, Transcript_1681	Reverse transcriptase (RNA-dependent DNA polymerase), Integrase core domain	gag-pol
	balancing sel	CLocus_57351	TRINITY_DN11166_c0_g3	Transcript_60243	no sig. HMMER hits	MAP3K
	balancing sel	CLocus_23794	TRINITY_DN12242_c0_g1	Transcript_63993, Transcript_63996	Reverse transcriptase (RNA-dependent DNA polymerase), Integrase core domain	pro-pol-dUTPase
	balancing sel	CLocus_376757	TRINITY_DN147102_c0_g1	Transcript_187547	PUB domain	PUB domain-containing protein
	balancing sel	CLocus_461127	TRINITY_DN20193_c1_g1	Transcript_85677	Reverse transcriptase (RNA-dependent DNA polymerase)	POL

622

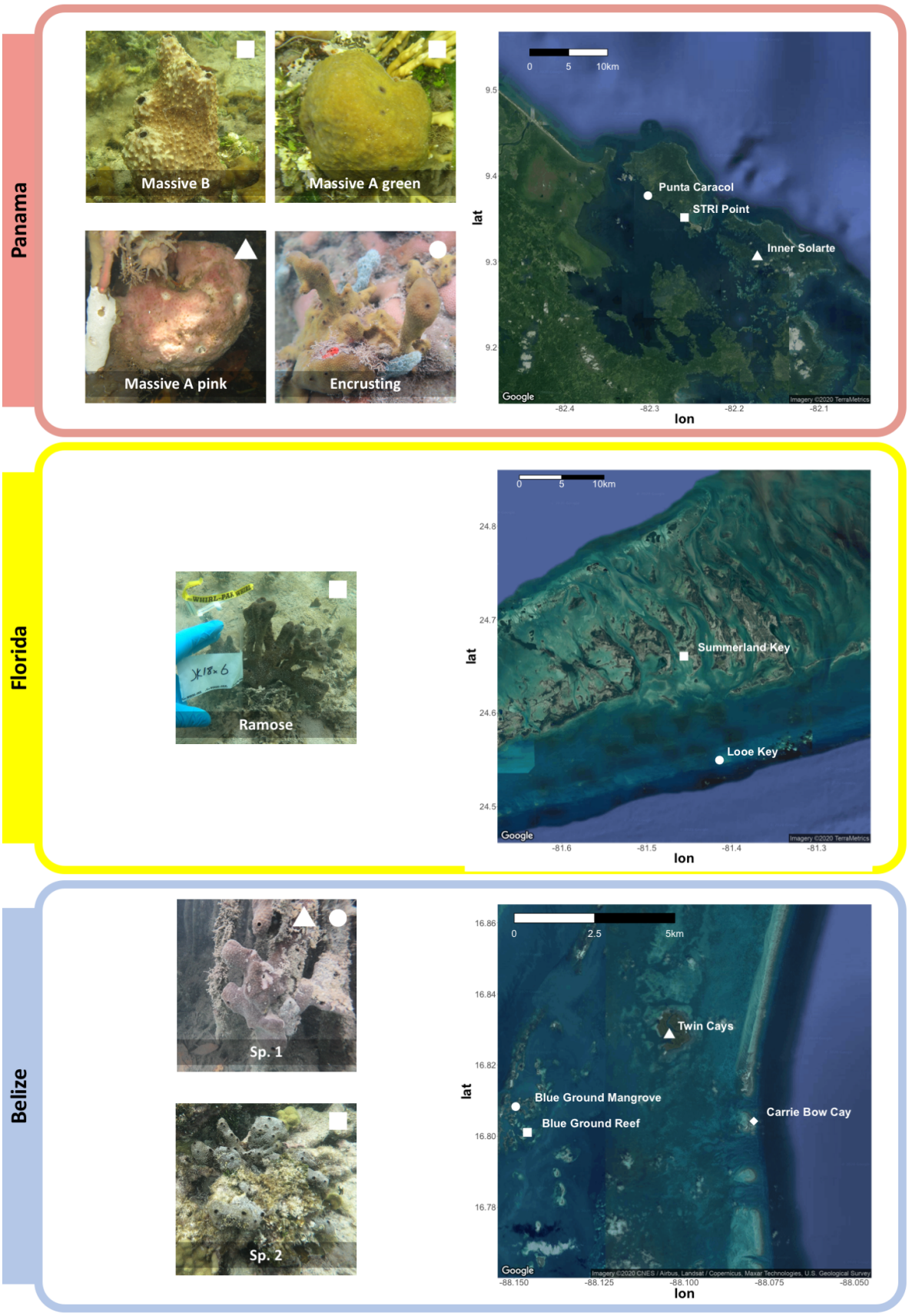
Panama
Massive B
Massive A green
Massive A pink
Encrusting
0 5 10km
Punta Caracol
STRI Point
Inner Solarte
lat
lon
Florida
Ramose
Summerland Key
Looe Key
Belize
Sp. 1
Sp. 2
Twin Cays
Blue Ground Mangrove
Blue Ground Reef
Carrie Bow Cay

623

624 **Figure 1. Specimens of *Ircinia* growth forms were sourced from three sites in the**
625 **Caribbean.**

626

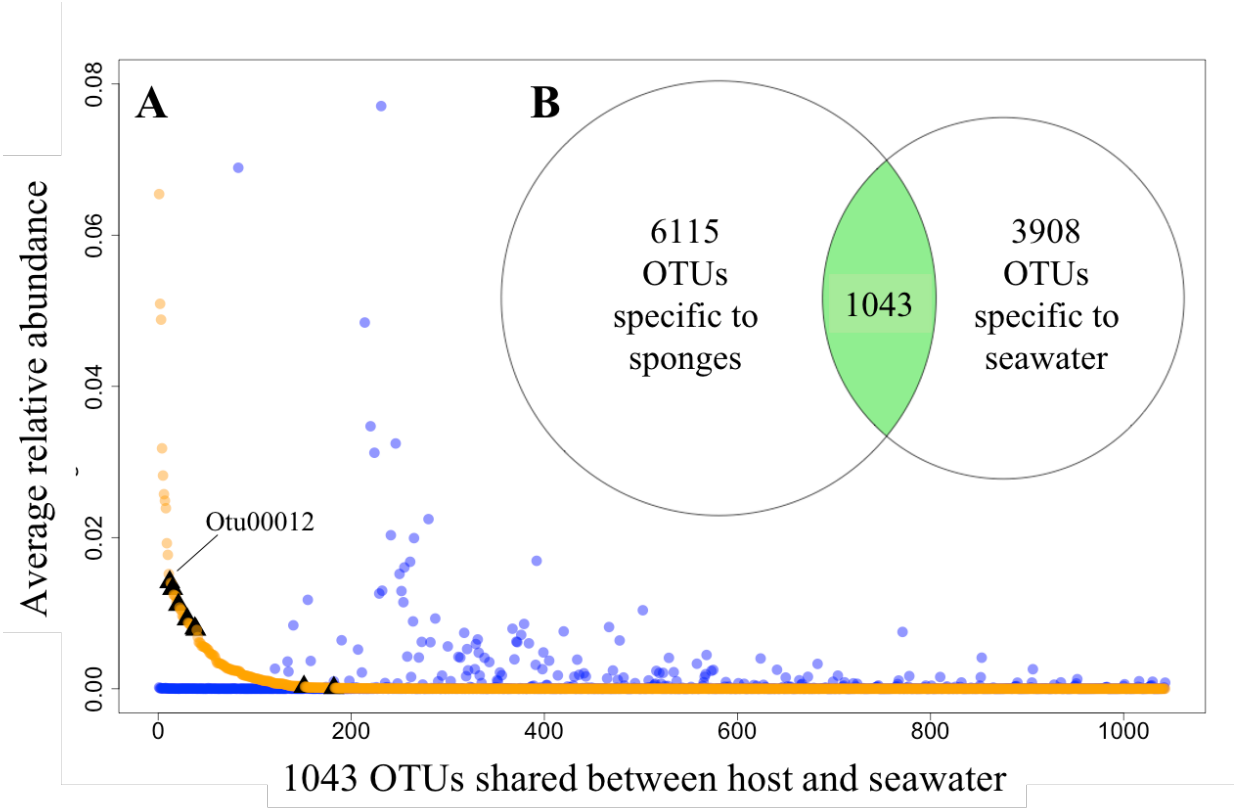

627

628 **Figure 2. *Ircinia* possess microbiomes that are compositionally distinct relative to microbial**
629 **communities of the ambient seawater**.

630

631

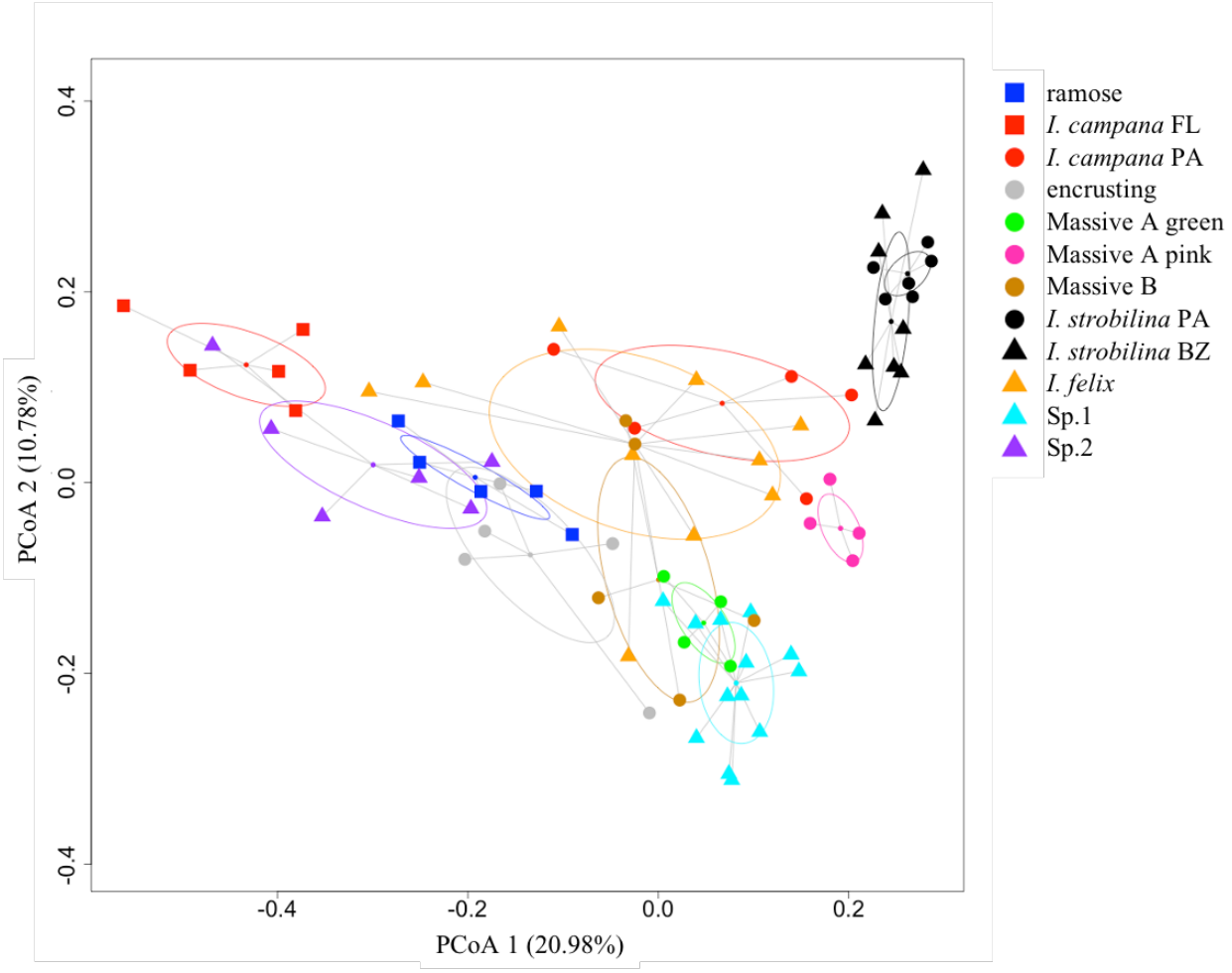

632

633 **Figure 3. Microbiome compositions are distinct among host lineages of *Ircinia.***

634

635

636

637

638

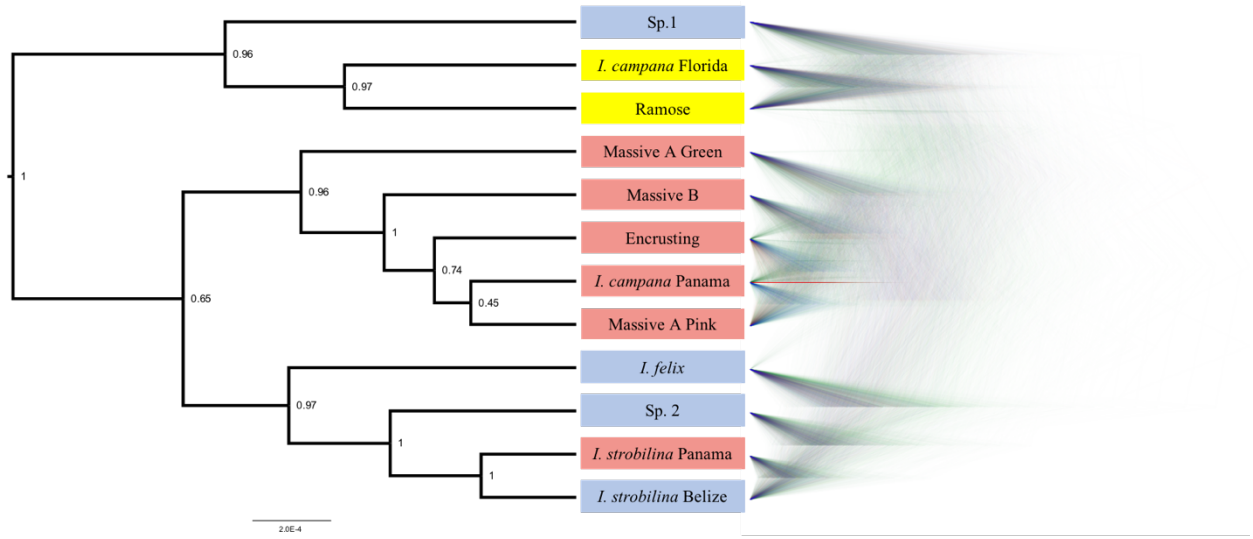

639

640 **Figure 4. The *Ircinia* growth forms are supported as being genetically distinct species**.

641

642

643

644

645

646

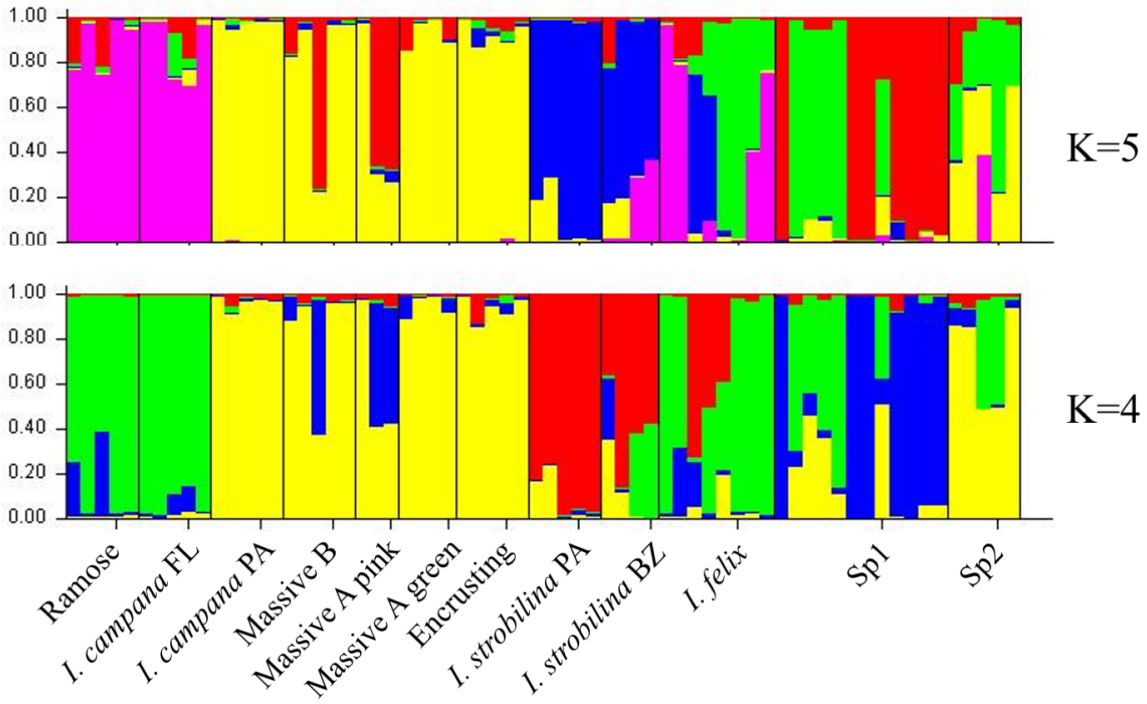

Figure 5. *Ircinia* experience high rates of hybridization within a site.

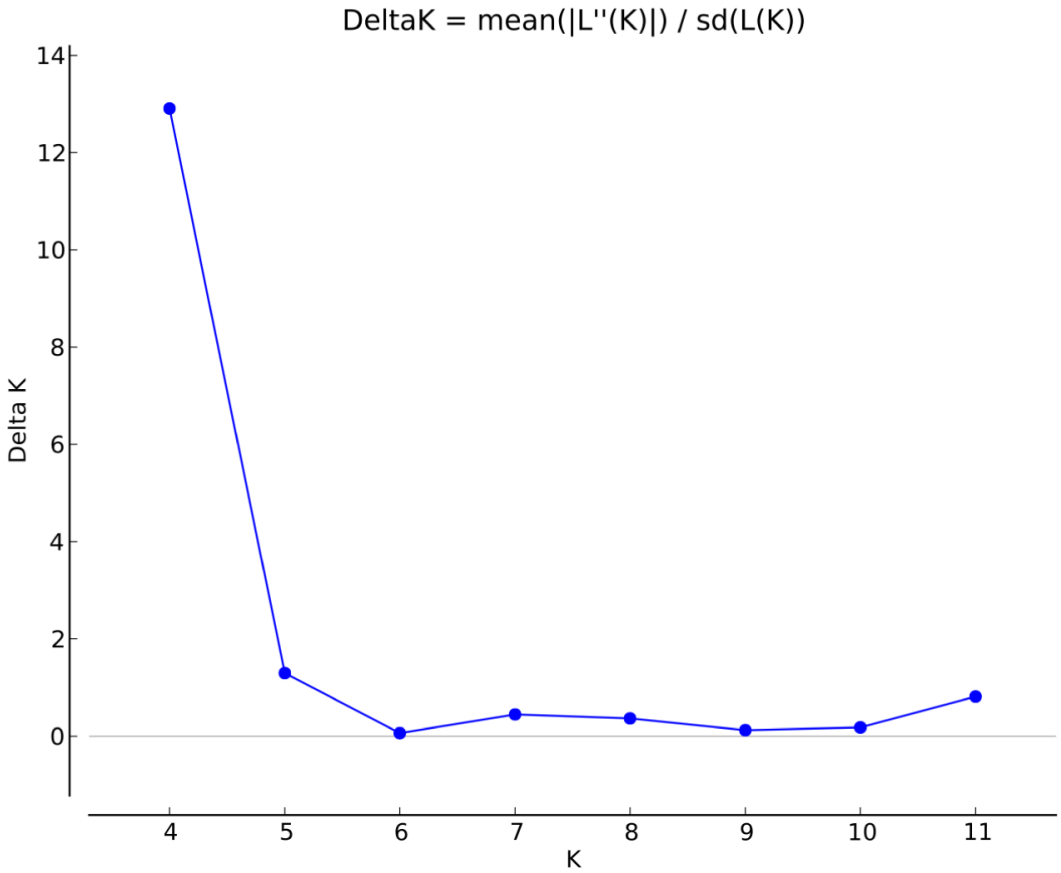

Figure S1. K=4 ancestral populations of *Ircinia* receive highest support via the Evanno method, followed by K=5.

668 **References**

669 1. Haney CH, Samuel BS, Bush J, Ausubel FM. 2015 Associations with rhizosphere bacteria
670 can confer an adaptive advantage to plants. *Nat. Plants* **1**, 15051.
671 (doi:10.1038/nplants.2015.51)

672 2. Berendsen RL, Pieterse CMJ, Bakker PAHM. 2012 The rhizosphere microbiome and
673 plant health. *Trends Plant Sci.* **17**, 478–486. (doi:10.1016/j.tplants.2012.04.001)

674 3. Clemente JC, Ursell LK, Parfrey LW, Knight R. 2012 The Impact of the Gut Microbiota
675 on Human Health: An Integrative View. *Cell* **148**, 1258–1270.
676 (doi:10.1016/j.cell.2012.01.035)

677 4. Freeman CJ, Thacker RW. 2011 Complex interactions between marine sponges and their
678 symbiotic microbial communities. *Limnol. Oceanogr.* **56**, 1577–1586.
679 (doi:10.4319/lo.2011.56.5.1577)

680 5. Moran NA, Baumann P. 2000 Bacterial endosymbionts in animals. *Curr. Opin. Microbiol.*
681 **3**, 270–275. (doi:https://doi.org/10.1016/S1369-5274(00)00088-6)

682 6. Falkowski PG, Dubinsky Z, Muscatine L, Porter JW. 1984 Light and the Bioenergetics of
683 a Symbiotic Coral. *Bioscience* **34**, 705–709. (doi:10.2307/1309663)

684 7. Long SR. 1989 Rhizobium-legume nodulation: Life together in the underground. *Cell* **56**,
685 203–214. (doi:https://doi.org/10.1016/0092-8674(89)90893-3)

686 8. Yeoman CJ, White BA. 2014 Gastrointestinal Tract Microbiota and Probiotics in
687 Production Animals. *Annu. Rev. Anim. Biosci.* **2**, 469–486. (doi:10.1146/annurev-animal-
688 022513-114149)

689 9. Brown SP, Cornforth DM, Mideo N. 2012 Evolution of virulence in opportunistic
690 pathogens: generalism, plasticity, and control. *Trends Microbiol.* **20**, 336–342.
691 (doi:10.1016/j.tim.2012.04.005)

692 10. Kiers ET, Rousseau RA, West SA, Denison RF. 2003 Host sanctions and the legume–
693 rhizobium mutualism. *Nature* **425**, 78–81. (doi:10.1038/nature01931)

694 11. Aderem A, Underhill DM. 1999 Mechanisms of Phagocytosis in Macrophages. *Annu. Rev.*
695 *Immunol.* **17**, 593–623. (doi:10.1146/annurev.immunol.17.1.593)

696 12. Nyholm S V, McFall-Ngai M. 2004 The winnowing: establishing the squid–vibrio
697 symbiosis. *Nat. Rev. Microbiol.* **2**, 632–642. (doi:10.1038/nrmicro957)

698 13. Wiens M, Korzhev M, Perovic-Ottstadt S, Luthringer B, Brandt D, Klein S, Muller WEG.
699 2007 Toll-like receptors are part of the innate immune defense system of sponges
700 (demospongiae: Porifera). *Mol. Biol. Evol.* **24**, 792–804. (doi:10.1093/molbev/msl208)

701 14. Sweet MJ, Hume DA. 1996 Endotoxin signal transduction in macrophages. *J. Leukoc.*
702 *Biol.* **60**, 8–26. (doi:10.1002/jlb.60.1.8)

703 15. Böhm M, Hentschel U, Friedrich A, Fieseler L, Steffen R, Gamulin V, Müller I, Müller
704 W. 2001 Molecular response of the sponge Suberites domuncula to bacterial infection.
705 *Mar. Biol.* **139**, 1037–1045. (doi:10.1007/s002270100656)

706 16. Dunn CW, Leys SP, Haddock SHD. 2015 The hidden biology of sponges and
707 ctenophores. *Trends Ecol. Evol.* **30**, 282–291. (doi:10.1016/j.tree.2015.03.003)

708 17. Brunton FR, Dixon OA. 1994 Siliceous sponge-microbe biotic associations and their
709 recurrence through the Phanerozoic as reef mound constructors. *Palaios* **9**, 370–387.
710 (doi:10.2307/3515056)

711 18. Vacelet J, Donadey C. 1977 *Vacelet J, Donadey C.. Electron microscope study of the*
712 *association between some sponges and bacteria. J Exp Mar Biol Ecol 30: 301-314*.
713 (doi:10.1016/0022-0981(77)90038-7)

714 19. Wilkinson CR. 1978 Microbial associations in sponges. II. Numerical analysis of sponge
715 and water bacterial populations. *Mar. Biol.* **49**, 169–176. (doi:10.1007/BF00387116)

716 20. Hentschel U, Usher KM, Taylor MW. 2006 Marine sponges as microbial fermenters.
717 *FEMS Microbiol. Ecol.* **55**, 167–177. (doi:10.1111/j.1574-6941.2005.00046.x)

718 21. Thomas T *et al.* 2016 Diversity, structure and convergent evolution of the global sponge
719 microbiome. *Nat. Commun.* **7**, 11870.

720 22. Thomas TRA, Kavlekar DP, LokaBharathi PA. 2010 Marine drugs from sponge-microbe
721 association--a review. *Mar. Drugs* **8**, 1417–1468. (doi:10.3390/md8041417)

722 23. Tian R-M, Wang Y, Bougouffa S, Gao Z-M, Cai L, Bajic V, Qian P-Y. 2014 Genomic
723 analysis reveals versatile heterotrophic capacity of a potentially symbiotic sulfur-oxidizing
724 bacterium in sponge. *Environ. Microbiol.* **16**, 3548–3561. (doi:10.1111/1462-2920.12586)

725 24. Archer SK, Stevens JL, Rossi RE, Matterson KO, Layman CA. 2017 Abiotic conditions
726 drive significant variability in nutrient processing by a common Caribbean sponge, Ircinia
727 felix. *Limnol. Oceanogr.* **62**, 1783–1793. (doi:10.1002/lno.10533)

728 25. Slaby BM, Hackl T, Horn H, Bayer K, Hentschel U. 2017 Metagenomic binning of a
729 marine sponge microbiome reveals unity in defense but metabolic specialization. *Nat.*
730 *Publ. Gr.* **11**, 2465–2478. (doi:10.1038/ismej.2017.101)

731 26. Rix L, Ribes M, Coma R, Jahn MT, de Goeij JM, van Oevelen D, Escrig S, Meibom A,
732 Hentschel U. 2020 Heterotrophy in the earliest gut: a single-cell view of heterotrophic
733 carbon and nitrogen assimilation in sponge-microbe symbioses. *ISME J.*
734 (doi:10.1038/s41396-020-0706-3)

735 27. Achlatis M, Pernice M, Green K, Guagliardo P, Kilburn MR, Hoegh-Guldberg O, Dove S.
736 2018 Single-cell measurement of ammonium and bicarbonate uptake within a
737 photosymbiotic bioeroding sponge. *ISME J.* **12**, 1308–1318. (doi:10.1038/s41396-017-
738 0044-2)

739 28. Erwin PM, Thacker RW. 2008 Phototrophic nutrition and symbiont diversity of two

740 Caribbean sponge – cyanobacteria symbioses. (doi:10.3354/meps07464)

741 29. Wilson MC *et al.* 2014 An environmental bacterial taxon with a large and distinct
742 metabolic repertoire. *Nature* **506**, 58–62. (doi:10.1038/nature12959)

743 30. Lackner G, Peters EE, Helfrich EJN, Piel J. 2017 Insights into the lifestyle of uncultured
744 bacterial natural product factories associated with marine sponges. *Proc. Natl. Acad. Sci.*
745 **114**, E347 LP-E356. (doi:10.1073/pnas.1616234114)

746 31. Moitinho-Silva L *et al.* 2017 The sponge microbiome project. *Gigascience* **6**, 1–7.
747 (doi:10.1093/gigascience/gix077)

748 32. Freeman CJ, Easson CG, Matterson KO, Thacker RW, Baker DM, Paul VJ. 2020
749 Microbial symbionts and ecological divergence of Caribbean sponges: A new perspective
750 on an ancient association. *ISME J.* (doi:10.1038/s41396-020-0625-3)

751 33. Erwin PM, Pita L, López-Legentil S, Turon X. 2012 Stability of sponge-associated
752 bacteria over large seasonal shifts in temperature and irradiance. *Appl. Environ.*
753 *Microbiol.* **78**, 7358–7368. (doi:10.1128/AEM.02035-12)

754 34. Marino C, Pawlik J, Lopez-Legentil S, Erwin P. 2017 Latitudinal variation in the
755 microbiome of the sponge Ircinia campana correlates with host haplotype but not anti-
756 predatory chemical defense. *Mar. Ecol. Prog. Ser.* **565**, 53–66. (doi:10.3354/meps12015)

757 35. Griffiths S, Antwis R, Lenzi L, Lucaci A, Behringer DC, Butler M, Preziosi R. 2019 Host
758 genetics and geography influence microbiome composition in the sponge Ircinia campana.
759 *J. Anim. Ecol.* **88**, 1684–1695. (doi:10.1111/1365-2656.13065)

760 36. Van Soest RWM *et al.* 2019 World Porifera Database. (doi:10.14284/359)

761 37. Pita L, Turon X, López-Legentil S, Erwin PM. 2013 Host rules: spatial stability of
762 bacterial communities associated with marine sponges (Ircinia spp.) in the Western
763 Mediterranean Sea. *FEMS Microbiol. Ecol.* **86**, 268–276. (doi:10.1111/1574-6941.12159)

764 38. Wilkinson C, Cheshire A. 1990 Comparisons of sponge populations across the Barrier
765 Reefs of Australia and Belize: evidence for higher productivity in the Caribbean. *Mar.*
766 *Ecol. Prog. Ser.* **67**, 285–294. (doi:10.3354/meps067285)

767 39. Weisz JB, Hentschel U, Lindquist N, Martens CS. 2007 Linking abundance and diversity
768 of sponge-associated microbial communities to metabolic differences in host sponges.
769 *Mar. Biol.* **152**, 475–483. (doi:10.1007/s00227-007-0708-y)

770 40. Schloss PD *et al.* 2009 Introducing mothur: open-source, platform-independent,
771 community-supported software for describing and comparing microbial communities.
772 *Appl. Environ. Microbiol.* **75**, 7537–7541. (doi:10.1128/AEM.01541-09)

773 41. Anderson MJ. 2005 PERMANOVA Permutational multivariate analysis of variance.
774 *Austral Ecol.* (doi:10.1139/cjfas-58-3-626)

775 42. Jackson AL, Parnell AC, Inger R, Bearhop S. 2011 Comparing isotopic niche widths

among and within communities: SIBER – Stable Isotope Bayesian Ellipses in R. *J. Anim. Ecol.* , 595–602.

43. Bolger AM, Lohse M, Usadel B. 2014 Genome analysis Trimmomatic : a flexible trimmer for Illumina sequence data. *Bioinformatics* **30**, 2114–2120. (doi:10.1093/bioinformatics/btu170)

44. Quast C, Pruesse E, Yilmaz P, Gerken J, Schweer T, Yarza P, Peplies J, Glöckner FO. 2013 The SILVA ribosomal RNA gene database project: Improved data processing and web-based tools. *Nucleic Acids Res.* **41**, D590–D596. (doi:10.1093/nar/gks1219)

45. Yamada K, Fukuda W, Kondo Y, Miyoshi Y, Atomi H, Imanaka T. 2011 Constrictibacter antarcticus gen. nov., sp. nov., a cryptoendolithic micro-organism from Antarctic white rock. *Int. J. Syst. Evol. Microbiol.* **61**, 1973–1980. (doi:10.1099/ijs.0.026625-0)

46. Flanagan SP, Jones AG. 2017 Constraints on the FST–Heterozygosity Outlier Approach. *J. Hered.* **108**, 561–573. (doi:10.1093/jhered/esx048)

47. Foll M, Gaggiotti O. 2008 A Genome-Scan Method to Identify Selected Loci Appropriate for Both Dominant and Codominant Markers: A Bayesian Perspective. *Genetics* **180**, 977 LP – 993. (doi:10.1534/genetics.108.092221)

48. Wood DE, Salzberg SL. 2014 Kraken: ultrafast metagenomic sequence classification using exact alignments. *Genome Biol.* **15**, R46. (doi:10.1186/gb-2014-15-3-r46)

49. Schmieder R, Edwards R. 2011 Fast identification and removal of sequence contamination from genomic and metagenomic datasets. *PLoS One* **6**, e17288. (doi:10.1371/journal.pone.0017288)

50. Martin M. 2011 CUTADAPT removes adapter sequences from high-throughput sequencing reads. *EMBnet.journal* **17**. (doi:10.14806/ej.17.1.200)

51. Catchen J, Hohenlohe PA, Bassham S, Amores A, Cresko WA. 2013 Stacks: an analysis tool set for population genomics. *Mol. Ecol.* **22**, 3124–3140. (doi:10.1111/mec.12354)

52. Grabherr MG *et al.* 2011 Full-length transcriptome assembly from RNA-Seq data without a reference genome. *Nat. Biotechnol.* (doi:10.1038/nbt.1883)

53. Scott C. 2016 dammit: an open and accessible de novo transcriptome annotator. *in prep.*

54. Leaché AD, Fujita MK, Minin VN, Bouckaert RR. 2014 Species delimitation using genome-wide SNP Data. *Syst. Biol.* **63**, 534–542. (doi:10.1093/sysbio/syu018)

55. Kass RE, Raftery AE. 1995 Bayes Factors. *J. Am. Stat. Assoc.* **90**, 773–795. (doi:10.1080/01621459.1995.10476572)

56. Evanno G, Regnaut S, Goudet J. 2005 Detecting the number of clusters of individuals using the software STRUCTURE: a simulation study. *Mol. Ecol.* **14**, 2611–2620. (doi:10.1111/j.1365-294X.2005.02553.x)

57. Liu L, Yu L, Kubatko L, Pearl DK, Edwards S V. 2009 Coalescent methods for estimating

812 phylogenetic trees. *Mol. Phylogenet. Evol.* **53**, 320–328.
813 (doi:https://doi.org/10.1016/j.ympev.2009.05.033)

814 58. Schmitt S, Weisz JB, Lindquist N, Hentschel U. 2007 Vertical transmission of a
815 phylogenetically complex microbial consortium in the viviparous sponge Ircinia felix.
816 *Appl. Environ. Microbiol.* **73**, 2067–2078. (doi:10.1128/AEM.01944-06)

817 59. Lee OO, Chui PY, Wong YH, Pawlik JR, Qian P-Y. 2009 Evidence for vertical
818 transmission of bacterial symbionts from adult to embryo in the Caribbean sponge
819 Svenzea zeai. *Appl. Environ. Microbiol.* **75**, 6147–6156. (doi:10.1128/AEM.00023-09)

820 60. Sharp KH, Eam B, Faulkner DJ, Haygood MG. 2007 Vertical Transmission of Diverse
821 Microbes in the Tropical Sponge Corticium sp. *Appl. Environ.*
822 *Microbiol.* **73**, 622 LP – 629. (doi:10.1128/AEM.01493-06)

823 61. Enticknap JJ, Kelly M, Peraud O, Hill RT. 2006 Characterization of a culturable
824 alphaproteobacterial symbiont common to many marine sponges and evidence for vertical
825 transmission via sponge larvae. *Appl. Environ. Microbiol.* **72**, 3724–3732.
826 (doi:10.1128/AEM.72.5.3724-3732.2006)

827 62. Erwin PM, Thacker RW. 2007 Incidence and identity of photosynthetic symbionts in
828 Caribbean coral reef sponge assemblages. *J. Mar. Biol. Assoc. United Kingdom* **87**, 1683–
829 1692. (doi:10.1017/S0025315407058213)

830 63. Glasl B, Smith CE, Bourne DG, Webster NS. 2018 Exploring the diversity-stability
831 paradigm using sponge microbial communities. *Sci. Rep.* **8**, 8425. (doi:10.1038/s41598-
832 018-26641-9)

833 64. Ferrer-Admetlla A *et al.* 2008 Balancing Selection Is the Main Force Shaping the
834 Evolution of Innate Immunity Genes. *J. Immunol.* **181**, 1315 LP – 1322.
835 (doi:10.4049/jimmunol.181.2.1315)

836 65. Leiva C, Taboada S, Kenny NJ, Combosch DJ, Giribet G, Jombart T, Riesgo A. 2019
837 Population substructure and signals of divergent adaptive selection despite admixture in
838 the sponge Dendrilla antarctica from shallow waters surrounding the Antarctic Peninsula.
839 *Mol. Ecol.* **28**, 3151–3170.

840 66. Orton RJ, Sturm OE, Vyshemirsky V, Calder M, Gilbert DR, Kolch W. 2005
841 Computational modelling of the receptor-tyrosine-kinase-activated MAPK pathway.
842 *Biochem. J.* **392**, 249–261. (doi:10.1042/BJ20050908)

843 67. Vos MD, Ellis CA, Bell A, Birrer MJ, Clark GJ. 2000 Ras Uses the Novel Tumor
844 Suppressor RASSF1 as an Effector to Mediate Apoptosis. *J. Biol. Chem.* **275**, 35669–
845 35672. (doi:10.1074/jbc.C000463200)

846 68. Agathanggelou A, Cooper WN, Latif F. 2005 Role of the Ras-Association Domain Family
847 1 Tumor Suppressor Gene in Human Cancers. *Cancer Res.* **65**, 3497 LP – 3508.
848 (doi:10.1158/0008-5472.CAN-04-4088)

849 69. Donninger H, Vos MD, Clark GJ. 2007 The RASSF1A tumor suppressor. *J. Cell Sci.* **120**,

850 3163 LP – 3172. (doi:10.1242/jcs.010389)

851 70. Stark MS *et al.* 2011 Frequent somatic mutations in MAP3K5 and MAP3K9 in metastatic
852 melanoma identified by exome sequencing. *Nat. Genet.* **44**, 165–169.
853 (doi:10.1038/ng.1041)

854 71. Coutts AS, MacKenzie E, Griffith E, Black DM. 2003 TES is a novel focal adhesion
855 protein with a role in cell spreading. *J. Cell Sci.* **116**, 897–906. (doi:10.1242/jcs.00278)

856 72. Manton KJ, Douglas ML, Netzel-Arnett S, Fitzpatrick DR, Nicol DL, Boyd AW,
857 Clements JA, Antalis TM. 2005 Hypermethylation of the 5' CpG island of the gene
858 encoding the serine protease Testisin promotes its loss in testicular tumorigenesis. *Br. J.*
859 *Cancer* **92**, 760–769. (doi:10.1038/sj.bjc.6602373)

860 73. Li X *et al.* 2014 Histone demethylase KDM5B is a key regulator of genome stability.
861 *Proc. Natl. Acad. Sci.* **111**, 7096 LP – 7101. (doi:10.1073/pnas.1324036111)

862 74. Brachner A *et al.* 2012 The endonuclease Ankle1 requires its LEM and GIY-YIG motifs
863 for DNA cleavage in vivo. *J. Cell Sci.* **125**, 1048–1057. (doi:10.1242/jcs.098392)

864 75. Dunin-Horkawicz S, Feder M, Bujnicki JM. 2006 Phylogenomic analysis of the GIY-YIG
865 nuclease superfamily. *BMC Genomics* **7**, 98. (doi:10.1186/1471-2164-7-98)

866 76. Suzuki T, Yasui M, Honma M. 2016 Mutator Phenotype and DNA Double-Strand Break
867 Repair in BLM Helicase-Deficient Human Cells. *Mol. Cell. Biol.* **36**, 2877–2889.
868 (doi:10.1128/MCB.00443-16)

869 77. Kalinovskaya NI *et al.* 1995 Surfactin-like structures of five cyclic depsipeptides from the
870 marine isolate of Bacillus pumilus. *Russ. Chem. Bull.* **44**, 951–955.
871 (doi:10.1007/BF00696935)

872 78. Prokof'eva NG, Kalinovskaya NI, Luk'yanov PA, Shentsova EB, Kuznetsova TA. 1999
873 The membranotropic activity of cyclic acyldepsipeptides from bacterium Bacillus
874 pumilus, associated with the marine sponge Ircinia sp. *Toxicon* **37**, 801–813.
875 (doi:10.1016/s0041-0101(98)00219-0)

876 79. Hardoim CCP, Costa R. 2014 Microbial communities and bioactive compounds in marine
877 sponges of the family Irciniidae-a review. *Mar. Drugs* **12**, 5089–5122.
878 (doi:10.3390/md12105089)

879 80. Jahn M *et al.* 2019 A Phage Protein Aids Bacterial Symbionts in Eukaryote Immune
880 Evasion. *Cell Host Microbe* **26**. (doi:10.1016/j.chom.2019.08.019)

881 81. González-Morales N, Holenka TK, Schöck F. 2017 Filamin actin-binding and titin-
882 binding fulfill distinct functions in Z-disc cohesion. *PLOS Genet.* **13**, e1006880.

883 82. Leber Y, Ruparelia AA, Kirfel G, van der Ven PFM, Hoffmann B, Merkel R, Bryson-
884 Richardson RJ, Fürst DO. 2016 Filamin C is a highly dynamic protein associated with fast
885 repair of myofibrillar microdamage. *Hum. Mol. Genet.* **25**, 2776–2788.
886 (doi:10.1093/hmg/ddw135)

887 83. Mao Z, Nakamura F. 2020 Structure and Function of Filamin C in the Muscle Z-Disc. *Int.*
888 *J. Mol. Sci.* **21**. (doi:10.3390/ijms21082696)

889 84. Leys SP, Yahel G, Reidenbach MA, Tunnicliffe V, Shavit U, Reiswig HM. 2011 The
890 sponge pump: the role of current induced flow in the design of the sponge body plan.
891 *PLoS One* **6**, e27787–e27787. (doi:10.1371/journal.pone.0027787)

892 85. Hoffmann F, Røy H, Bayer K, Hentschel U, Pfannkuchen M, Brümmer F, de Beer D.
893 2008 Oxygen dynamics and transport in the Mediterranean sponge Aplysina aerophoba.
894 *Mar. Biol.* **153**, 1257–1264. (doi:10.1007/s00227-008-0905-3)

895 86. Guannel G, Arkema K, Ruggiero P, Verutes G. 2016 The Power of Three: Coral Reefs,
896 Seagrasses and Mangroves Protect Coastal Regions and Increase Their Resilience. *PLoS*
897 *One* **11**, e0158094.

898 87. Müller WEG, Müller IM. 2003 Origin of the Metazoan Immune System: Identification of
899 the Molecules and Their Functions in Sponges1. *Integr. Comp. Biol.* **43**, 281–292.
900 (doi:10.1093/icb/43.2.281)

901 88. Wang S, Meyer E, Mckay JK, Matz M V. 2012 2b-RAD: A simple and flexible method
902 for genome-wide genotyping. *Nat. Methods* **9**, 808–810. (doi:10.1038/nmeth.2023)

903 89. Chen S, Zhou Y, Chen Y, Gu J. 2018 Fastp: an ultra-fast all-in-one FASTQ preprocessor.
904 *Bioinformatics* **34**, i884–i890. (doi:10.1093/bioinformatics/bty560)

905 90. Rognes T, Flouri T, Nichols B, Quince C, Mahé F. 2016 VSEARCH: a versatile open
906 source tool for metagenomics. *PeerJ* **4**, e2584–e2584. (doi:10.7717/peerj.2584)

907 91. Oksanen AJ *et al.* 2016 Vegan: community ecology package.
908 *https://github.com/vegandevs/vegan* (doi:10.4135/9781412971874.n145)

909 92. Schmieder R, Edwards R. 2011 Quality control and preprocessing of metagenomic
910 datasets. *Bioinformatics* **27**, 863–864. (doi:10.1093/bioinformatics/btr026)

911 93. Paris JR, Stevens JR, Catchen JM. 2017 Lost in parameter space: a road map for stacks.
912 *Methods Ecol. Evol.* **8**, 1360–1373. (doi:10.1111/2041-210X.12775)

913 94. Beaumont MA, Nichols RA. 1996 Evaluating Loci for Use in the Genetic Analysis of
914 Population Structure. *Proc. R. Soc. London Ser. B* **263**, 1619–1626.

915 95. Bouckaert R, Heled J, Kühnert D, Vaughan T, Wu CH, Xie D, Suchard MA, Rambaut A,
916 Drummond AJ. 2014 BEAST 2: a software platform for Bayesian evolutionary analysis.
917 *PLoS Comput. Biol.* **10**, e1003537. (doi:10.1371/journal.pcbi.1003537)

918 96. Bryant D, Bouckaert R, Felsenstein J, Rosenberg NA, Roychoudhury A. 2012 Inferring
919 species trees directly from biallelic genetic markers : bypassing gene trees in a full
920 coalescent analysis. *Mol. Biol. Evol.* **29**, 1917–1932. (doi:10.1093/molbev/mss086)

921 97. Earl D, vonHoldt BM. 2011 STRUCTURE HARVESTER: a website and program for
922 visualizing STRUCTURE output and implementing the Evanno method. *Conserv. Genet.*

Resour. **4**, 359–361.